International Journal of Engineering (IJE)
Singaporean Journal of Scientific Research(SJSR)
Vol.6.No.5.2014 Pp.235-240
Available at:www.iaaet.org/sjsr
Paper Received:19-04-2014
Paper Accepted:24-04-2014
Paper Reviewed by:1Prof.Dr.Karthikeyan 2. Chai ChengYue

WIND AND SOLAR ENERGY CONVERSION SYSTEM USING MPPT BASED POWER ELECTRONICS

P.VENKATESAN, Dr.S.SENTHILKUMAR
VSB College of Engineering Technical Campus,
Electrical and Electronics Engineering, Salem, Tamilnadu, India.
brathikalai@gmail.com,sengce2009@yahoo.in

ABSTRACT

In this paper, High efficient boost- half-bridge photovoltaic (PV) microinverter system implemented by an *LLC* resonant dc–dc converter is proposed. In order to achieve low cost, easy control, high efficiency, and high reliability, a boost-half-bridge dc–dc converter using minimal devices is introduced to interface the low-voltage PV module. A full-bridge pulse width-modulated inverter is cascaded and injects synchronized sinusoidal current to the grid. A fourth-order linear- phase IIR filter is proposed to regulate the grid current. High power factor and very low total harmonic distortions are guaranteed under both heavy load and light load conditions. Variable step size is adopted such that fast tracking speed and high MPPT efficiency are both obtained. By frequency modulation control, the output impedance of an *LLC* converter can be regulated from zero to infinite without shunt or serial resistors. Therefore, the efficiency of the proposed boost-half-bridge photovoltaic (PV) microinverter system significantly increased. Simulation results are provided to verify the validity and performance of the circuit operations control, and MPPT algorithm.

***Keywords*—** LLC resonant dc–dc converter, Boost-half-bridge, grid-connected photovoltaic (PV) system, maximum power point tracking (MPPT).

I. INTRODUCTION

RECENTLY, residue of traditional energy resources (i.e., fossil energy) is highly limited and would be exhausted in the near future. Besides, combustion of fossil fuels results in a serious threat of global warming. Hence, developing renewable energy resources to replace traditional ones has been a research of great urgency. Among all renewable energy resources, pho- tovoltaic (PV) energy becomes most attractive recently, because it is noiseless, pollution-free, nonradioactive, and inexhaustible. Since the output PV characteristics are influenced by illumination and temperature, the maximum power point tracking (MPPT) [1], [2] is a necessary technology in PV applications. The concept of microinverter (also known as module- integrated converter/inverter) has become a future trend for single-phase grid-connected photovoltaic (PV) power systems for its removal of energy yield mismatches among PV modules, possibility of individual PV-module-oriented optimal design, independent maximum power point tracking (MPPT), and "plug and play" concept . In general, a PV microinverter system is often supplied by a low-voltage solar panel, which requires a high-voltage step-up ratio to produce desired output ac voltage [3]–[5]. Hence, a dc–dc converter cascaded by an inverter is the most popular topology, in which a HF transformer is often implemented within the dc–dc conversion stage [4]–[10].

In terms of the pulsewidth modulation (PWM) techniques employed by the PV microinverter system, two major categories are attracting most of the attentions. In the first, PWM control is applied to both the dc–dc converter and the inverter [4]–[6]. In addition, a constant voltage dc link decouples the power flow in the two stages such that the dc input is not affected by the double-line-frequency power

ripple appearing at the ac side. By contrast, the second configuration utilizes a quasi-sinusoidal PWM method to control the dc–dc converter in order to generate a rectified sinusoidal current (or voltage) at the inverter dc link. Accordingly, a line-frequency-commutated inverter un- folds the dc-link current (or voltage) to obtain the sinusoidal form synchronized with the grid [7]–[10]. Although the latter has the advantage of higher conversion efficiency due to the elimination of HF switching losses at the inverter, the double- line-frequency power ripple must be all absorbed by the dc input capacitor, making the MPPT efficiency (defined as the ratio of the energy drawn by the PV inverter within a certain measuring period at the steady state to the theoretical available energy from the PV module) compromised unless a very large capacitance is used. Moreover, the dc–dc conversion stage requires more challenging control techniques to meet the grid current regulation requirement. Therefore, in terms of the MPPT performance and output current quality, the first category of PV microinverter is more appropriate and will be adopted in this paper.

Atmospheric conditions are uncontrollable so that PV sys- tem engineers cannot obtain the corresponding PV characteristics to qualify the feasibility and dynamic response of their MPPT approaches immediately. Among them, the most applicable approach in high-power systems is using pulse width modulation (PWM) dc–dc converters to generate PV characteristics. However, shunt resistors are required to limit output voltage at extremely high duty-ratio, and serial resistors are used to inhibit spike current at extremely low duty-ratio operation. These resistors cause additional power dissipations and lower conversion efficiency. Furthermore, the power switches of PWM converters operate in hard switching, which will result in high switching losses and electromagnetic interference (EMI) issues.

This paper proposes to implement a high-efficiency boost-half-bridge photovoltaic (PV) microinverter system by an *LLC* dc–dc converter.

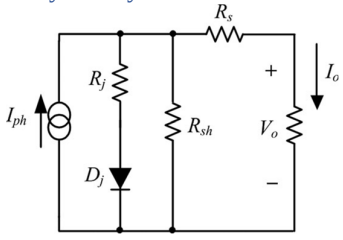

Fig. 1. Equivalent circuit of a solar cell.

II. CHARACTERISTICS OF SOLAR CELLS

Solar cells are basically p–n junction semiconductors which transform solar energy into electricity directly. Fig. 1 shows an equivalent circuit of a solar cell [2], in which R_{sh} and R_S are the intrinsic shunt and serial resistors of the cell, respectively. A current source I_{ph} represents the cell photocurrent, which is a function of illumination S_i and solar array temperature T, and can be expressed as follows:

$$I_{ph}= [I_{sso}+K_i(T-T_r)]S_i/100 \quad (1)$$

where I_{sso} is the short-circuit current at reference temperature T_r and reference illumination (100mW/cm^2), and K_i is temperature coefficient of the short-circuit current.

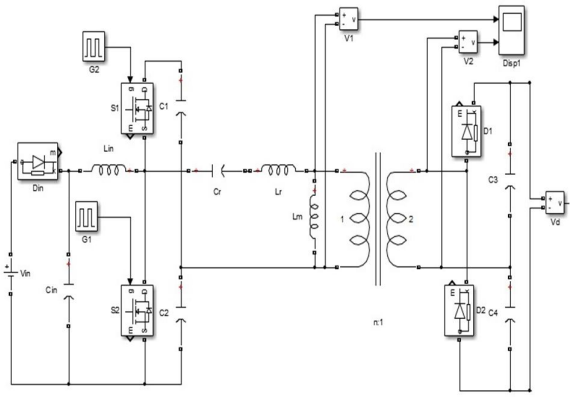

Fig. 2. Circuit diagram of *LLC* dc/dc converter.

III. ANALYSIS OF THE *LLC* DC–DC CONVERTER

The circuit diagram of an *LLC* dc–dc converter is shown in Fig. 2, which consists of an *LLC* inverter, a current-driven transformer with a rectifier. The topology of *LLC* converter is very similar to that of SRC. The main difference is that the magnetizing inductance L_m is only slightly higher than the resonant inductance L_r in the *LLC* converter. Therefore, at some load conditions, L_m may participate in the resonance with L_r and C_r and change the characteristics of resonant tank.

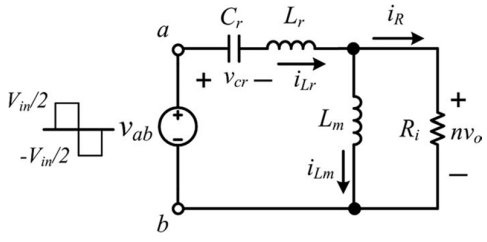

Fig. 3. Equivalent circuit of the *LLC* converter.

The equivalent circuit of the *LLC* inverter

can be depicted as shown in Fig. 3, in which R_i is equivalent load resistance seen in primary side, and can be expressed as $R_i=8n^2R_L/\pi^2$. The input symmetrical square waveform V_{ab} with the magnitude of $V_{in}/2$ can be obtained by alternate conducting of power switches S_1 and S_2. The load quality factor are defined as

$$A=L_r/L_m \quad (2)$$

$$\omega_L= 2\pi f_L \quad (3)$$

$$Q_L=Ri.\ \omega_L.C_r \quad (4)$$

Were ω_L is the resonance frequency

ω_H is the main resonance frequency

IV. BOOST-HALF-BRIDGE PV MICROINVERTER

In the front-end dc–dc converter, a conventional boost converter is modified by split- ting the output dc capacitor into two separate ones. C_{in} and L_{in} denote the input capacitor and boost inductor, respectively. The center taps of the two MOSFETs (S_1 and S_2) and the two output capacitors (C_1 and C_2) are connected to the primary terminals of the transformer T_r, just similar to a half bridge. A voltage doubler composed of two diodes (D_1 and D_2) and two capacitors (C_3 and C_4) is incorporated to rectify the transformer secondary voltage to the inverter dc link. A full-bridge inverter composed of four MOSFETs (S_3 –S_6) using synchronized PWM control serves as the dc–ac conversion stage. Sinusoidal current with a unity power factor is supplied to the grid through a third-order *LCL* filter (L_{o1}, L_{o2}, and C_o).

The transformer primary voltage, secondary voltage, and primary current are denoted as v_{r1}, v_{r2}, and i_r

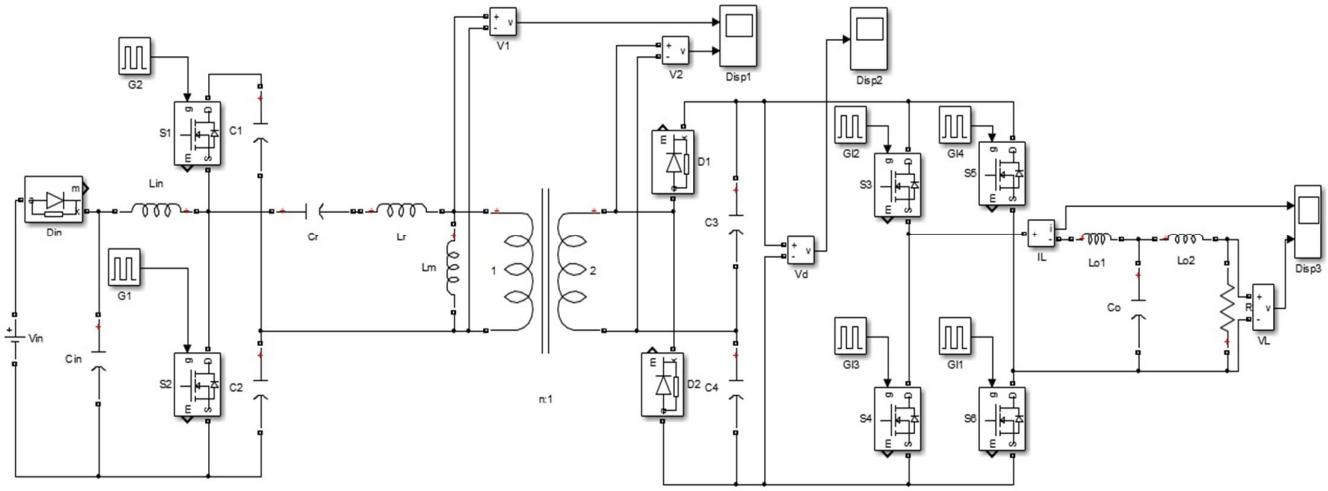

The boost-half-bridge microinverter topology for grid-connected PV systems is depicted in Fig. 4. It is composed of two decoupled power processing stages.

1, respectively.

Fig. 4. boost-half-bridge microinverter with LLC DC-DC converter

The boost-half-bridge converter is controlled by S_1 and S_2 with complementary duty cycles. Neglect all the switching dead bands for simplification. The idealized transformer operating waveforms are illustrated in Fig. 5. When S_1 is ON and S_2 is OFF, v_{r1} equals to v_{C1}. When S_1 is OFF and S_2 is ON, v_{r1} equals to $-v_{C2}$. At the steady state, the transformer volt-second is always automatically balanced. In other words, the primary volt-second A_1 (positive section) and A_2 (negative section) are equal, so are the secondary volt-sec A_3 (positive section) and A_4 (negative section).

In order to reach an optimal efficiency of the boost-half-bridge converter, ZVS techniques can be considered for practical implementation, as guided by [12]. It is worth noting that engineering tradeoffs must be made between the reduced switching losses and increased conduction losses when soft switching is adopted. Detailed optimal design processes of the boost-half-bridge con-verter will not be addressed in this paper.

For simplicity, hard switching is employed and the transformer leakage inductance is regarded as small enough in this paper.

The step-changed voltage reference and the ramp-changed volt- age reference are implemented for MPPT, respectively.

V. OPERATION PRINCIPLES OF THE *LLC* DC–DC CONVERTER

As shown in Fig. 2, the primary switches S_1 (S_2) are com- posed of an MOSFET Q_1 (Q_2), and its intrinsic antiparallel diode D_1 (D_2) and equivalent output capacitor C_{OSS1} (C_{OSS2}). The resonant tank is formed by the resonant capacitor C_r, and the leakage inductor L_r and magnetizing inductor L_m of the transformer T_1. By conducting the switches S_1 and S_2 alter- nately, a symmetrical square waveform with the magnitude of $V_{in}/2$ can be obtained in the input terminal of the resonant tank, where V_{in} is the input voltage. The center-tapped rectifier is constructed by connecting diodes D_3 and D_4 to the secondary windings of T_1. Based on the analysis of earlier section, the main theoretical waveforms of the *LLC* converter are shown in Fig.5.

VI.MPPT

Fig. 5 shows the voltage and current waveforms of the primary switches S_1 and S_2, when the system operates at the maximum power point (MPP) (point "E") and two extreme points (points "A" and "H"), respectively.

In order to further verify the system stability, a boost converter with perturb and observe (P&O) MPPT algorithm [1], [2] and output-current feedback control is connected in series with the proposed SYSTEM. This is one of the most popular structures to achieve MPPT feature in the PV applications. The impedance ratio, defined as $T_m = Z_o/Z_{in}$, can be used to determine the system stability, where Z_{in} is the input impedance of the boost converter.

VII. EXPERIMENTAL RESULTS

A boost-half-bridge PV microinverter has been built and simulated by MATLAB. The validity of the boost-half-bridge dc–dc converter, and the LLC DC-DC converter, and the variable step size MPPT method are verified by the following experimental results.

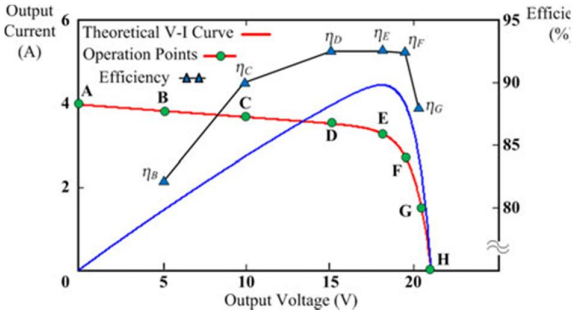

Fig. 5. Measured efficiencies of the proposed system according to the operation points "A" to "H."

Besides, when the System operates at point "E" with high-output power, the turn-off current can be reduced by the second resonance, as shown in Fig. 5. Therefore, the circulating energy and turn-off loss can be significantly minimized to improve system efficiency. Fig. 6 shows the measured efficiencies according to the operation points (from "A" to "H") marked at the theoretical *V–I* curve. The maximum system efficiency is up to around 92.5% and occurs at the MPP "E," resulting in energy saving significantly.

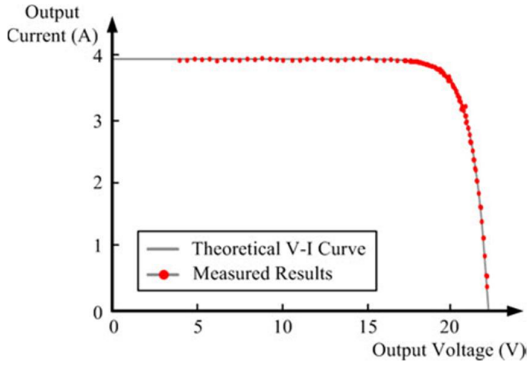

Fig. 6. Measured *V–I* curve of the proposed system with closed-loop control.

In Fig. 7. Shows that the Transformer primary voltage, secondary voltage and currents when without using *LLC* converter. In Fig. 8. Shows that the Transformer primary voltage, secondary voltage and currents when with using *LLC* converter.

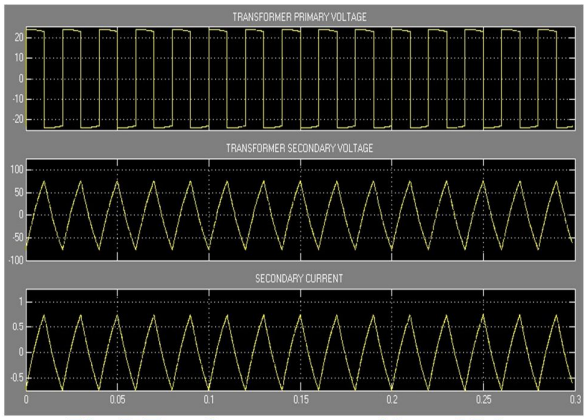

Fig. 7. Transformer output with out *LLC* converter.

From that Fig.7 & 8. We find that the output efficiency and quality of output getting improved when using the LLC DC-DC converter. While using this system we can get the smooth output waveform then the normal output.

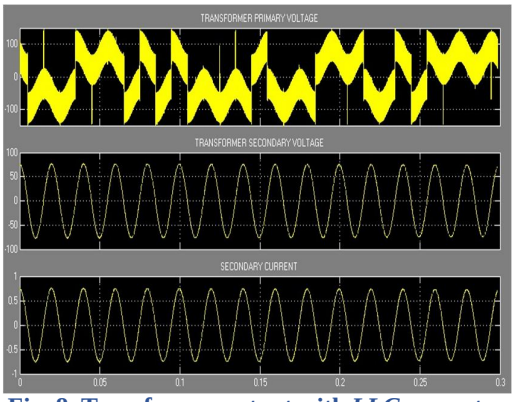

Fig. 8. Transformer output with *LLC* converter

In Fig. 9. Shows that the Output of boost-half-bridge microinverter system implemented by LLC DC-DC converter using MPPT.

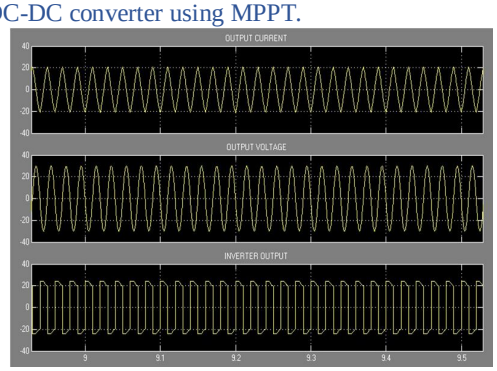

Fig. 8. Output of boost-half-bridge microinverter system

VII.CONCLUSION

A high-efficiency boost-half-bridge microinverter system implemented by LLC DC-DC converter using MPPT has been proposed. The detail operation principle, design procedures, and considerations are introduced. A simulation of boost-half-bridge microinverter system implemented by LLC DC-DC converter using MPPT is implemented to demonstrate the feasibility and validity of the theoretical discussion. The simulation results show that the boost-half-bridge microinverter system implemented by LLC DC-DC converter using MPPT can provide approximated PV output characteristics with high accuracy, and the maximum system efficiency at the range near MPP is up to around 92.5%. Hence, the proposed boost-half-bridge microinverter system implemented by LLC DC-DC converter using MPPT save the costs and energy for PV system testing, and accelerate the industrial developments of PV power.

Thanks to the minimal use of semiconductor devices, circuit simplicity, and easy control, the boost-half-bridge PV microinverter possesses promising features of low cost and high reliability. Finally, the customized MPPT method that generates a ramp-changed reference for the PV voltage regulation guarantees a correct and reliable operation of the PV microinverter system.

REFERENCES

[1] S. B. Kjaer, J. K. Pedersen, and F. Blaabjerg, "A review of single-phase grid-connected inverters for photovoltaic modules," *IEEE Trans. Ind. Appl.*, vol. 41, no. 5, pp. 1292–1306, Sep./Oct. 2005.

[2] Q. Li and P. Wolfs, "A review of the single phase photovoltaic module in- tegrated converter topologies with three different DC link configurations," *IEEE Trans. Power Electron.*, vol. 23, no. 3, pp. 1320–1333, May 2008.

[3] R. Wai and W. Wang, "Grid-connected photovoltaic generation system,"*IEEE Trans. Circuits Syst.-I*, vol. 55, no. 3, pp. 953–963, Apr. 2008.

[4] M. Andersen and B. Alvsten, "200 W low cost module integrated utility interface for modular photovoltaic energy systems," in *Proc. IEEE IECON*,1995, pp. 572–577.

[5] A. Lohner, T. Meyer, and A. Nagel, "A new panel-integratable inverter concept for grid-connected photovoltaic systems," in *Proc. IEEE Int. Symp. Ind. Electron.*, 1996, pp. 827–831.

[6] D. C. Martins and R. Demonti, "Grid connected PV system using two energy processing stages," in *Proc. IEEE Photovolt. Spec. Conf.*, 2002, pp. 1649–1652.

[7] T. Shimizu, K. Wada, and N. Nakamura, "Flyback-type single-phase utility interactive inverter with power pulsation decoupling on the dc input for an ac photovoltaic module system," *IEEE Trans. Power Electron.*, vol. 21, no. 5, pp. 1264–1272, Sep. 2006.

[8] N. Kasa, T. Iida, and L. Chen, "Flyback inverter controlled by sensorless current MPPT for photovoltaic power system," *IEEE Trans. Ind. Electron.*, vol. 52, no. 4, pp. 1145–1152, Aug. 2005.

[9] Q. Li and P. Wolfs, "A current fed two-inductor boost converter with an in- tegrated magnetic structure and passive lossless snubbers for photovoltaicmodule integrated converter applications," *IEEE Trans. Power Electron.*, vol. 22, no. 1, pp. 309–321, Jan. 2007.

[10] S. B. Kjaer and F. Blaabjerg, "Design optimization of a single phase inverter for photovoltaic applications," in *Proc. IEEE Power Electron.Spec. Conf.*, 2003, pp. 1183–1190.

[11] H. Li, F. Z. Peng, and J. S. Lawler, "Modeling, simulation, and exper- imental verification of soft-switched bi-directional dc-dc converters," in *Proc. IEEE Appl. Power Electron. Conf.*, 2001, pp. 736–742.

[12] F. Z. Peng, H. Li, G. Su, and J. S. Lawler, "A new ZVS bidirectional DC– DC converter for

fuel cell and battery application," *IEEE Trans. Power Electron.*, vol. 19, no. 1, pp. 54–65, Jan. 2004.

[13] H. Li and F. Z. Peng, "Modeling of a new ZVS bi-directional dc-dc converter," *IEEE Trans. Aerosp. Electron. Syst.*, vol. 40, no. 1, pp. 272–283, Jan. 2004.

[14] D. Liu and H. Li, "A ZVS bi-directional DC–DC converter for multiple energy storage elements," *IEEE Trans. Power Electron.*, vol. 21, no. 5, pp. 1513–1517, Sep. 2006.

[15] C. Yoon, J. Kim, and S. Choi, "Multiphase DC–DC converters using a boost-half-bridge cell for high-voltage and high-power applications,"*IEEE Trans. Power Electron.*, vol. 26, no. 2, pp. 381–388, Feb. 2011.

[16] K. Zhang, Y. Kang, J. Xiong, and J. Chen, "Direct repetitive control of SPWM inverters for UPS purpose," *IEEE Trans. Power Electron.*, vol. 18, no. 3, pp. 784–792, May. 2003.

[17] Y.-Y. Tzou, S.-L. Jung, and H.-C. Yeh, "Adaptive repetitive control of PWM inverters for very low THD AC-voltage regulation with unknown loads," *IEEE Trans. Power Electron.*, vol. 14, no. 5, pp. 973–981, Sep.1999.

[18] Y.-Y. Tzou, R.-S. Ou, S.-L. Jung, and M.-Y. Chang, "High-performance programmable AC power source with low harmonic distortion using DSP- based repetitive control technique," *IEEE Trans. Power Electron.*, vol. 12, no. 4, pp. 715–725, Jul. 1997.